Metamorphism and exhumation of the NW Himalaya constrained by U–Th–Pb analyses of detrital monazite grains from early foreland basin sediments

NIKKI M. WHITE[1], R. R. PARRISH[2], M. J. BICKLE[1], Y. M. R. NAJMAN[1,3,4], D. BURBANK[5]
& A. MAITHANI[6]

[1]*Department of Earth Sciences, Cambridge University, Downing Street, Cambridge CB2 3EQ, UK*
(e-mail: nicola@esc.cam.ac.uk)
[2]*NERC Isotope Geosciences Laboratory, Kingsley Dunham Centre, Keyworth, Nottingham NG12 5GG, UK*
[3]*Department of Geology and Geophysics, Edinburgh University, Grant Institute, Kings Buildings, West Mains Road,
Edinburgh EH9 3JW, UK*
[4]*Present address: Department of Geology and Geophysics, University of Calgary, 2500 University Drive,
NW Calgary, Canada*
[5]*Dept. of Geosciences, 539 Deike Building, Pennsylvania State University, University Park, PA 16802 USA*
[6]*Remote Sensing Lab., Geology Division KDM Instt. of Petroleum Exploration, Oil and Natural Gas Corporation,
Dehra Dun, 248 195 Uttar Pradesh, India*

Abstract: Single detrital monazite grains from the Dharamsala and Lower Siwalik Formations (early to mid-Miocene continental foreland basin sediments in NW India) have been dated by two techniques; isotope dilution thermal ionization multicollector mass spectrometry (ID-TIMS) and laser ablation plasma ionization multicollector mass spectrometry (LA-PIMMS). The results give U–Th–Pb isotopic ages of *c.* 400–1300 Ma and 28–37 Ma and suggest that the source of detritus shed from the uplifting Himalayan mountains and captured in the foreland basin included (1) the protolith to the High Himalayan Crystalline Series (HHCS), i.e. rocks unaffected by the Himalayan metamorphism, (2) Cambro-Ordovician granites and (3) HHCS affected by the M_1 phase of Barrovian metamorphism (Eo-Himalayan) related to the Indo-Asian collision. Deposition of the Dharamsala Formation was coeval with M_2 sillimanite grade Himalayan metamorphism and crustal melting.

The youngest monazite (*c.* 28–37 Ma) ages imply that Indian plate rocks, having experienced the earliest Himalayan metamorphic event which occurred within 10–20 Ma of collision were exhumed, eroded and deposited within *c.* 10–20 Ma of metamorphism. This indicates a minimum cooling rate of between 60 and $40°C\ Ma^{-1}$ for the period 30–20 Ma. After 20 Ma our study suggests no change in source area and that this same sequence, comprising both metamorphosed and unmetamorphosed rocks, was supplying detritus and being progressively incised by erosion for at least a further 8 million years.

Keywords: Himalayas, Siwalik Range, monazite, exhumation, foreland basins.

Synorogenic sediments preserve information about the past kinematics and exhumation of mountain belts, a history that in the mountain chain itself is largely overprinted by later metamorphism and deformation, or removed by erosion. In this paper we use U–Th–Pb ages of detrital monazite grains from the Himalayan Miocene foreland basin sediments to understand better their sources and the timing of metamorphism and exhumation in the Himalayas. The kinematic evolution of the Himalaya, particularly the timing of the movement on the major faults, is still poorly constrained despite the significance of the Himalayan–Tibetan region as the prime example of an active collisional orogen (Avouac & Tapponnier 1993).

Monazite is an LREE phosphate accessory phase with a high closure temperature (>750°C) so that U–Th–Pb ages generally date growth of the mineral during amphibolite-facies conditions in metamorphic rocks or crystallization from anatectic melts (Spear & Parrish 1996; Simpson *et al.* 2000). We use the ages of single grains analysed by whole-grain dissolution and isotope dilution thermal ionization mass-spectrometry (ID-TIMS) as well as by spot analyses by laser ablation plasma ionization multicollector mass spectrometry (LA-PIMMS). The monazites analysed in this study give both Mesoproterozoic to Lower Palaeozoic (pre-collisional) and Tertiary (post-collisional) ages. The mineral ages allow identification of the tectonic units being eroded, the timing of metamorphic events and the exhumation history of the metamorphic rocks. The speed and adequate precision of the LA-PIMMS method is well suited to analysis of detrital mineral populations and allows recovery of polyphase histories from monazite grains which have grown in multiple episodes.

Geological and metamorphic evolution

The Himalayas result from the collision of Tibetan continental crust (Lhasa Block) and the mid-Cretaceous to Palaeocene Trans-Himalayan batholith, with the northern margin of the Indian continental plate (Hodges 2000). The Indian plate rocks include late Archaean, Proterozoic and Phanerozoic continental margin sequences (Fig. 1). The Indus–Tsangpo suture zone, the site of the collision, contains ophiolites and flysch (Searle 1983; Garzanti & Van Haver 1988). These were thrust south
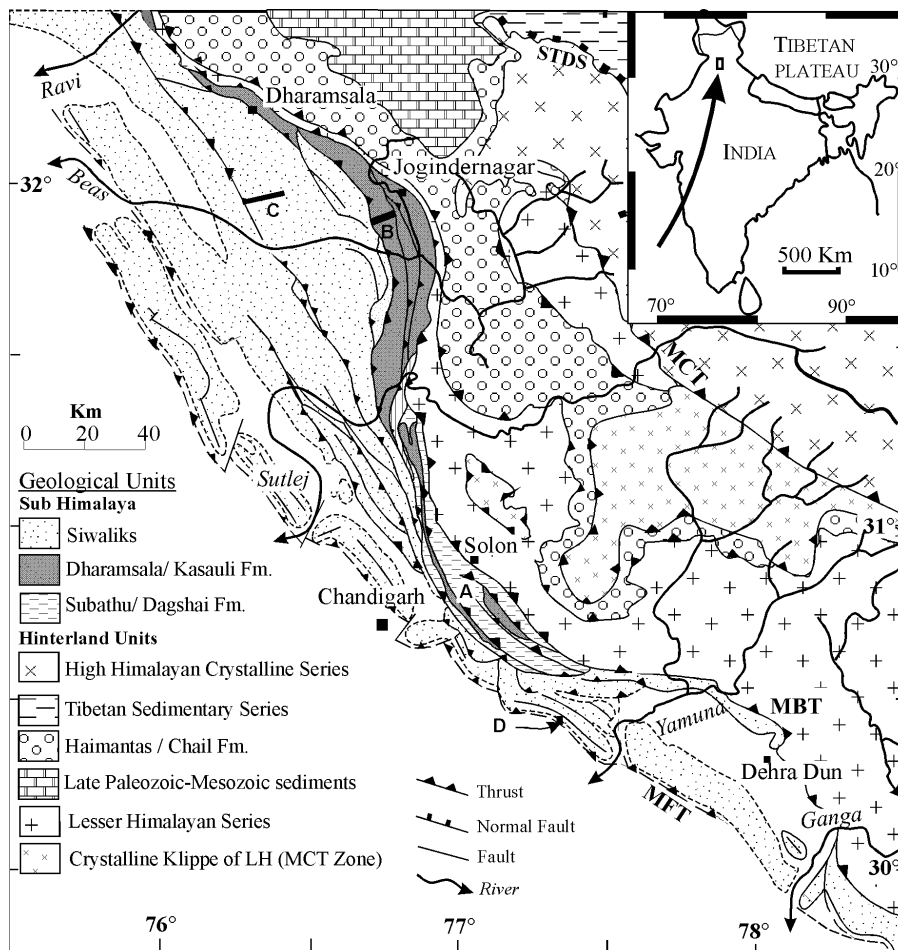
Fig. 1. Geological map of North Indian Sub-Himalaya, inset shows location of map (boxed). Sections A–D refer to Fig. 2. Section B south of Jogindernagar shows this location of this study. Major Himalayan faults are marked; STDS, South Tibetan Detachment System; MCT, Main Central Thrust; MBT, Main Boundary Thrust; MFT, Main Frontal Thrust. Map is adapted from Powers *et al.* (1998), Karunakaran & Ranga Rao (1979), Raiverman *et al.* (1983) and Thakur (1998).

onto the north Indian passive continental margin which comprises a fold and thrust belt of Proterozoic metasediments and Cambro-Ordovician granitiods, and Palaeozoic and Mesozoic sediments of the Tibetan Sedimentary Series (Fuchs 1982; Gaetani & Garzanti 1991). These rocks provided the protolith for the medium and high grade migmatites, leucogranites and gneisses of the High Himalayan Crystalline Series (Le Fort *et al.* 1987; Pognante *et al.* 1990; Hodges 2000 and references therein). The High Himalayan Crystalline Series are separated from the underlying Tibetan Sedimentary Series by the South Tibetan Detachment System of low-angle north dipping normal faults active from *c.* 22 Ma to 16 Ma or younger (e.g. Searle *et al.* 1997; Dezes *et al.* 1999; Walker *et al.* 1999). The metamorphic rocks of the High Himalayan Crystalline Series are thrust over the lower grade rocks of the Lesser Himalayan Series by the Main Central Thrust. The timing of the Main Central Thrust is complicated but is thought to be around 23–20 Ma (Hubbard & Harrison 1989; Hodges *et al.* 1996). However $^{39}Ar/^{40}Ar$ biotite ages of *c.* 4 Ma (Copeland *et al.* 1991), K–Ar muscovite ages of *c.* 6 Ma (Metcalfe 1993), and Th–Pb monazite ages of *c.* 6 Ma in garnet-grade rocks within the high strain zone of the Main Central Thrust are interpreted as the reactivation of this fault *c.* 8–6 Ma and imply 20 km of exhumation since then (Harrison *et al.* 1997). The Lesser Himalayan Series, which comprises unmetamorphosed or low-grade Paleoproterozoic metasediments with volcanic and granitic components (Valdiya 1980; Valdiya & Bhatia 1980), has a distinctly older crustal source with whole-rock $\varepsilon_{Nd} \approx -25$ and detrital zircon ages between 1800 and 2600 Ma,

compared with the High Himalayan Crystalline Series which were derived from Meso-Neoproterozoic crust with $\varepsilon_{Nd} \approx -16$ and detrital zircons between 800 and 1000 Ma (France-Lanord *et al.* 1993; Parrish & Hodges 1996; Ahmad *et al.* 2000). The Lesser Himalayas has been thrust over the Sub-Himalayas, comprising Palaeogene and Neogene units of the foreland basin, along the Main Boundary Thrust initiated by *c.* 10 Ma (Meigs *et al.* 1995). The Sub-Himalaya is emplaced over the youngest units of the foreland basin sediments along the presently active Main Frontal Thrust.

The Indian continental crust first collided with Asia at *c.* 50 Ma (Rowley 1996). Subsequently, southward-propagating folding and thrusting of the Indian margin thickened the crust and resulted in mid-Eocene to early Oligocene Barrovian Eo-Himalayan metamorphism. The oldest direct isotopic dates on this event are monazite and zircon ages of *c.* 35 Ma from a kyanite leucosome in Nepal (Godin *et al.* 1999), 32 Ma monazite from a sillimanite-bearing metapelitic gneiss from the Everest region (Simpson *et al.* 2000), Sm–Nd garnet–whole-rock ages on kyanite grade rocks of *c.* 40 Ma from Garhwal (Prince *et al.* 1999), and Sm–Nd garnet core and rim ages between 33 and 27 Ma from Zanskar (Vance & Harris 1999). The latter ages combined with *P–T–t* path determinations (Vance & Mahar 1998) show that the Zanskar High Himalayan Crystalline crust was being buried between 35 and 25 Ma. After 25 Ma the High Himalayan Crystalline rocks now exposed at the surface underwent decompression (decompression segments of clockwise *P–T–t* loops are reported widely across the Himalayas; Guillot *et al.* 1999) and many

mineral cooling ages (K–Ar, ^{39}Ar/^{40}Ar and Rb–Sr on micas and ^{39}Ar/^{40}Ar on hornblende) lie in the period 25–15 Ma. Harris & Ayres (1998) argue that rapid decompression caused the fluid-absent melting responsible for the Himalayan leucogranites intruded between c. 24 and 12 Ma (Searle et al. 1997; Walker et al. 1999).

The classic view of Himalayan evolution distinguishes the 40–30 Ma 'Eo-Himalayan' metamorphism from the post-25 Ma 'Neo-Himalayan' metamorphism associated with decompression, melting, leucogranite intrusion and mineral cooling ages (e.g. Hodges 2000). However the P–T–t paths suggest that these metamorphic events are part of one cycle of burial, pro-grade heating followed by decompression and exhumation to the surface. One of the major questions concerning Himalayan evolution is whether this metamorphic cycle affected all the High Himalayan rocks sequentially such that a major section of the crust was first buried, heated and finally uplifted by movement of the Main Central Thrust. Alternatively, crustal thickening, burial, and uplift is a diachronous, semi-continuous process accommodated along southward propagation structures. If the metamorphic and tectonic processes are 'semi-continuous' then all parts of the P–T–t cycle would be operating simultaneously with northern parts of the orogen being uplifted through the high-T, low-P field prior to exhumation whilst southern parts of the belt are being overthrusted and buried. These arguments have implications for the developement of the inverted metamorphic sequence seen in the Main Central Thrust zone and High Himalayan Crystalline Series (cf. Stephenson et al. 2000). The presence within the Main Central Thrust high strain zone of much younger metamorphic rocks with P–T paths distinct from the High Himalayas in several localities implies substantial exhumation, and by implication, movement and southward propagation on the Main Central Thrust since 10 Ma (Harrison et al. 1997; Stephenson et al. 2000). We use the detrital monazite ages presented below to place additional constraints on the metamorphic evolution.

The foreland basin

The foreland basin occupies much of the Indus, Ganges and Brahmaputra river basins that are still the sites of sediment accumulation. Older units are exposed by thrusting of the Sub-Himalaya above the Main Frontal Thrust (Fig. 1). The oldest rocks in the Sub-Himalaya are Palaeocene to early mid-Eocene (lower Lutetian) carbonate deposits with a low clastic input and detrital mineralogy and Nd–Sr isotopic systematics characteristic of Indus–Tsangpo suture zone rocks (Mathur 1978; Najman & Garzanti 2000; Najman et al. 2000) (Fig. 2). Eocene and lower Oligocene rocks are largely lacking while upper Oligocene, Miocene and younger rocks are continental fluvial, lacustrine or deltaic sediments. The restricted regional extent of the deposits, their exposure as a thrust complex and the difficulty of correlation in what are largely unfossiliferous rocks has led to a plethora of local formation names. In NW India the Oligocene–Miocene succession has been variously termed the Dharamsalas (Chaudhri 1975; Raiverman & Seshavataram 1965; Raiverman et al. 1983) or divided into the older Dagshai and overlying Kasauli Formations (Raiverman et al. 1983; Najman et al. 1993). Detrital mica ages date units in the Dagshai Formation as younger than 28 Ma and 25 Ma and two units in the Kasauli Formation as younger than 28 Ma and a third unit as younger
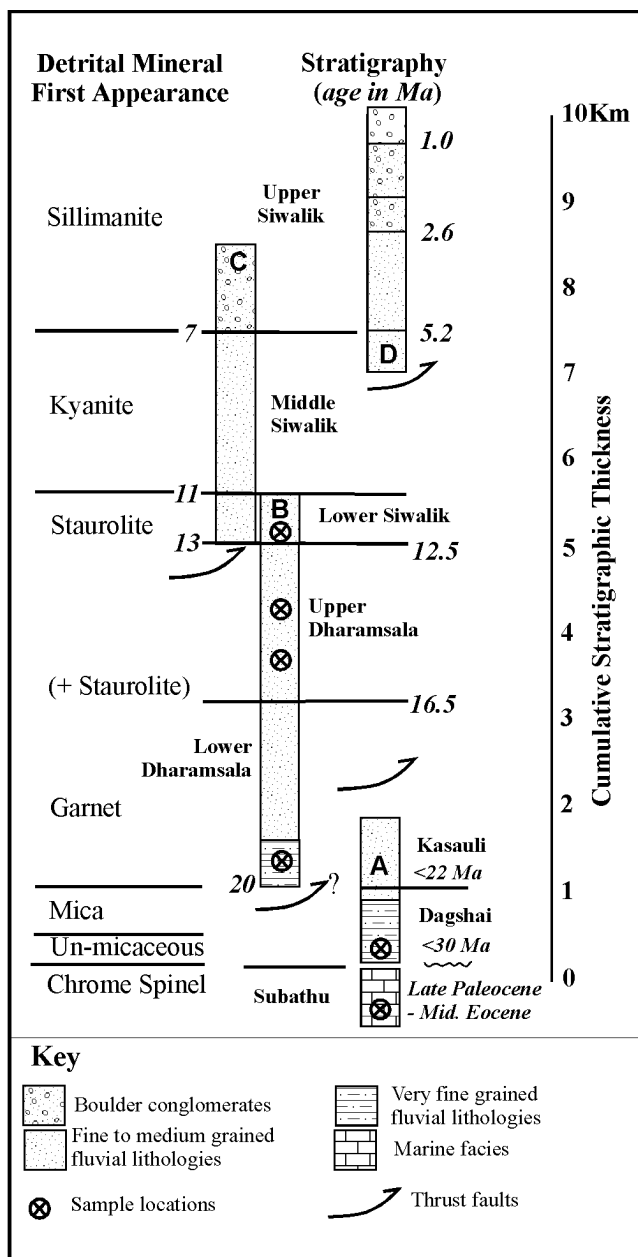

Fig. 2. Simplified correlation of Indian foreland stratigraphy with first appearance (or absence) of minerals; chrome spinel in the Subathu shows ophiolitic/suture influence (Najman & Garzanti 2000). From Dagshai to Upper Siwalik the grade of detrital metamorphic minerals increases indicating progressive unroofing of the hinterland (Chaudhri 1975). Sections are (A) Raiverman & Seshavataram (1965) ages based on mica dating Najman et al. (1997), (B) this study, Chimnun–Birdhar section of Raiverman & Seshavataram (1965), magnetostratigraphic ages, (C) Jawalamukhi section, Meigs et al. (1995), magnetostratigraphic ages, (D) Jamni–Khola section, Sangode et al. (1996) magnetostratigraphy & fauna. Locations as Fig. 1. Crossed circles show samples prepared for this study.

than 22 Ma (Najman et al. 1997) (Fig. 2). The section sampled for this study is from the Dharamsalas and Lower Siwaliks near Jogindernagar where the section is dated by magnetostratigraphy to between 20 and 12 Ma (Fig. 3). The formations consist of fine- to medium-grained fluvial sandstones, siltstones
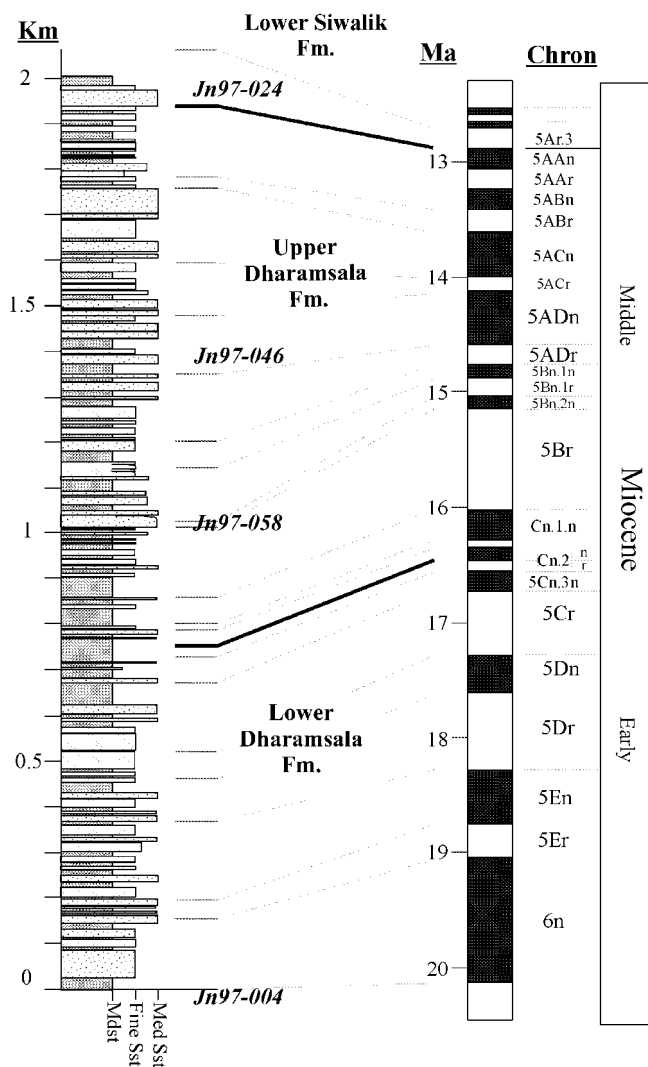
Fig. 3. Simplified stratigraphic log of the Dharamsala Formation of NW India based on measured sections on the Neri–Jogindernagar road (Fig. 1) (Birdhar–Chimnun section of Raiverman & Seshavataram 1965) showing the position of samples selected for analysis. The correlated magnetostratigraphy is the unpublished data of Maithani and Burbank. Magnetic reversal time scale after Cande & Kent (1995).

and overbank mudstones with abundant caliche soil formation, fossil leaves and logs. The base of the section is a thrust fault overlying Siwalik sediments. There is no evidence of the marine facies Subathu Fm.

The Middle Miocene to Lower Pleistocene fluvial Siwalik formations crop out along the entire 2400 km foothills of the Himalaya (Gansser 1964) with depositional ages established by extensive magnetostratigraphy, ash horizons and mammalian fauna (Burbank 1996). Fluvial deposition continues today in the foreland belt.

Analytical methods

Sample preparation

Four fluvial sandstone samples were collected from a >2000 m section of Lower Dharamsala to Lower Siwalik rocks for which a magneto-stratigraphic section of Maithani and Burbank (unpublished data)

constrain depositional age (Figs 1 & 3). The samples have depositional ages of *c.* 20 Ma (JN97-004), 15 Ma (JN97-058), 14.5 Ma (JN97-046) and *c.* 12.8 Ma (JN97-024) (Fig. 3). Samples were crushed, sieved to 255 μm, put through heavy liquids and heavy minerals were separated magnetically. Zircon and monazite were handpicked (>80 μm) on the basis of size and clarity. Samples of sandstone from the underlying Dagshai formation (Hm97-17A) and the Subathu formation (Hm98-14A) were prepared in a similar way but yielded no monazite grains (Fig. 2).

ID-TIMS

Single-grain dating using whole-grain dissolution and ID-TIMS employed methods similar to Parrish *et al.* (1987) and Noble *et al.* (1993), and used a Daly photomultiplier ion counting system, supplemented in part by multiple faraday cup collection of the larger ion beams, on a VG 354 instrument. A ^{205}Pb–^{233}U–^{235}U spike was used, allowing normalization of U isotopic measurements for increased accuracy and precision. The Pb and U blanks for the samples were approximately 6 and 1 picogram, respectively. The REE eluant from the ion chromatography was saved for analysis of the Nd and Sm isotopes (White *et al.* 2000). U–Pb data are summarized in Table 1 and Fig. 4.

LA-PIMMS

During the course of this study, the U–Th–Pb laser ablation plasma ionization multicollector mass spectrometry (LA-PIMMS) capability was developed at the NERC Isotope Geosciences Laboratory using the recently acquired VG Elemental Plasma 54 instrument. Early in this development effort, a number of crystals from samples of this study were analysed in parallel with monazite mineral standards of known age. Monazite grains were mounted in FEP Teflon® and ground to expose an internal surface, then polished. Monazite standards were mounted in separate grain mounts and both were put into the laser cell and analysed using the VG P54 ICP multicollector mass spectrometer using methods of Parrish *et al.* (1999). A prototype VG Laserprobe II 266 nm NdYag laser attached to a computer-controlled X–Y–Z stage was used to ablate monazite crystals by a rectangular rastering method which sampled a volume of approximately $40 \times 40 \times 30$ μm within several grains using a laser beam spot diameter of about 15 μm. Thallium dissolved in nitric acid was first desolvated using a Cetac MCN 6000 nebulizer was introduced into the laser system, via argon carrier gas, to carry the ablated particles into the P54 plasma. The thallium serves as a precise monitor of instrumental mass bias. Data collection included Tl, Pb, U and Th isotopes, and a monitor of Hg interference on Pb. The measurement of the very small ^{204}Pb peak was made on the axial faraday cup, but in general it could not be differentiated from background, so that no common Pb correction was subsequently made. Measured Pb/U and Pb/Th ratios were compared to the same ratios constrained by TIMS on monazite standards. During the course of the study, 16 standards were measured that bracketed samples; these standards included both *c.* 54 Ma and 1876 Ma monazite crystals. When plotted as measured against known ratios, the standard data form a line with zero intercept, slope within 15% of unity. Changes to instrumental parameters affect the slope of this line, and when analyses were normalized during similar conditions, the uncertainty on the calibration was approximately 3–5% (1 σ) on Pb/U and Pb/Th. ^{207}Pb/^{206}Pb measurement precision depends upon signal intensity but can be as low as 0.1%. Table 2 and Fig. 5 shows the U–Th–Pb data and analytical errors. In some cases, the signal intensity of one or more Pb isotopes fell below the threshold of reliability which we regard as 0.16 mV of signal using 10^{11} resistors on faraday cups. In such cases only ratios with intensities exceeding this value are reported.

Results

Monazite grains are rare (<20 per sample) in comparison with zircon and other harder detrital minerals. Single grains of monazite picked from the samples weighed from 1–7 μg and

Table 1. *U-Pb ID-TIMS analytical data*

Fraction*	Wt (μg)	U (ppm)	Pb (ppm)	$^{206}Pb/^{204}Pb$‡	Pbc (pg)§	Th/U†	$^{206}Pb/^{238}U$¶	$^{207}Pb/^{235}U$¶	$^{207}Pb/^{206}Pb$¶	Age (Ma) $^{206}Pb/^{238}U$¶	Age (Ma) $^{207}Pb/^{235}U$¶	Age (Ma) $^{207}Pb/^{206}Pb$¶	ρ
JN97-004 Sandstone from base of Lower Dharamsala formation (c. 20 Ma)													
m-1 wr	3.1	1909	2160	2972	23	18	0.1850 (0.28)	1.9636 (0.28)	0.07696 (0.12)	1094 ± 5.5	1103 ± 3.8	1120 ± 4.8	0.91
m-2 wr	3	1643	3509	475.6	99	50	0.1492 (0.75)	1.4341 (0.85)	0.06970 (0.33)	896.7 ± 13.0	903.3 ± 10.0	919.5 ± 13.5	0.92
m-3 wr	1.8	4838	2394	3659	24	8.3	0.1592 (0.14)	1.5603 (0.16)	0.07108 (0.07)	952.4 ± 2.6	954.6 ± 2.0	959.6 ± 3.0	0.89
m-4 sa	3	9825	113.7	460.7	24	3.8	0.0059 (1.10)	0.0375 (1.70)	0.04616 (1.00)	37.8 ± 0.8	37.3 ± 1.2	6 ± 48.0	0.83
r-5	3.3	9.857	0.5765	43.17	5	0.25	0.0593 (2.60)	0.5712 (7.90)	0.06988 (6.60)	371.3 ± 19.0	458.8 ± 58.0	924.7 ± 275	0.62
JN97-058A Sandstone from Upper Dharamsala formation (c. 15 Ma)													
m-2 sa	6.7	11913	114.5	934.5	25	4.3	0.0046 (0.19)	0.0285 (0.28)	0.04514 (0.19)	29.41 ± 0.1	28.49 ± 0.2	−48.2 ± 9.4	0.76
m-3 sa	4.7	7453	90.76	546.4	18	6.9	0.0043 (0.20)	0.0276 (0.41)	0.04632 (0.32)	27.83 ± 0.1	27.68 ± 0.2	14.4 ± 15.0	0.66
JN97-046 Sandstone from Upper Dharamsala formation (c. 14.5 Ma)													
m-1 wr	1.9	3950	3799	12470	6	20	0.1561 (0.33)	1.5394 (0.33)	0.07153 (0.08)	935 ± 5.8	946.3 ± 4.1	972.6 ± 3.1	0.97
m-2 wr	1.8	3534	51.72	196.6	10	8.1	0.0046 (0.34)	0.0288 (1.60)	0.04520 (1.40)	29.7 ± 0.2	28.85 ± 0.9	−45 ± 69.0	0.51
m-3 sa	1.6	2186	3593	1956	18	36	0.1578 (0.40)	1.5411 (0.42)	0.07085 (0.17)	944.3 ± 6.9	946.9 ± 5.1	953.1 ± 7.0	0.91
m-4 r	2.2	298.2	1537	680.8	7	157	0.1197 (0.41)	1.0588 (0.55)	0.06418 (0.43)	728.6 ± 5.6	733.3 ± 5.7	747.5 ± 18.0	0.64
z-1 euh	3.3	326.1	44.66	1298	7	0.18	0.1403 (0.37)	1.3164 (0.59)	0.06807 (0.55)	846.2 ± 5.9	853 ± 6.9	870 ± 22.7	0.44
z-2 sm	4.3	270.5	37.8	1298	8	0.27	0.1407 (1.50)	1.3952 (1.10)	0.07190 (1.20)	848.8 ± 23.3	886.9 ± 14.0	983.1 ± 47.9	0.62
JN97-024 Sandstone from the base of the Lower Siwalik formation (c. 12.8 Ma)													
m-2 wr	1.5	1923	2621	2920	6	50	0.0941 (0.15)	0.7629 (0.17)	0.05878 (0.10)	580 ± 1.1	575.7 ± 1.5	558.8 ± 4.5	0.79
m-3 r	2.4	1736	3066	3213	13	37	0.1631 (0.16)	1.6232 (0.18)	0.07220 (0.08)	973.7 ± 2.9	979.2 ± 2.2	991.6 ± 3.2	0.9
m-4 sr	2.3	4692	3557	3356	31	15	0.1557 (0.14)	1.5124 (0.17)	0.07050 (0.06)	932.6 ± 2.5	935.4 ± 2.0	941.9 ± 2.6	0.93
m-6 wr	2.4	3996	4117	2308	37	23	0.1439 (0.57)	1.3742 (0.61)	0.06928 (0.16)	866.4 ± 9.2	878 ± 7.1	907.1 ± 6.6	0.97
m-7 sr	5.1	129.2	1797	397	24	240	0.2193 (0.41)	2.6588 (0.54)	0.08795 (0.34)	1278 ± 9.5	1317 ± 8.0	1381 ± 13.1	0.78
m-8 sr	2.5	1712	4897	1250	37	59	0.1742 (0.34)	1.7697 (0.39)	0.07369 (0.21)	1035 ± 6.6	1034.4 ± 5.1	1033.1 ± 8.5	0.84

*M, monazite, Z, zircon, R,rutile; all single grain analysis; wr, well rounded; r, rounded; sr, sub-rounded; sa, sub-angular; euh, euhudral; sm, smooth.
†Atomic ratio of Th to U, calculated from radiogenic $^{208}Pb/^{206}Pb$.
‡Measured ratio, corrected for spike and Pb fractionation (0.13%/amu).
§Total common Pb in analysis, corrected for fractionation and spike.
¶Corrected for blank Pb and U, and common Pb (Stacey-Kramers model Pb equivalent to interpreted age of mineral); errors are 1 standard error of the mean in percent for ratios and 2 standard errors of the mean when expressed in Ma. ρ Correlation coefficient.
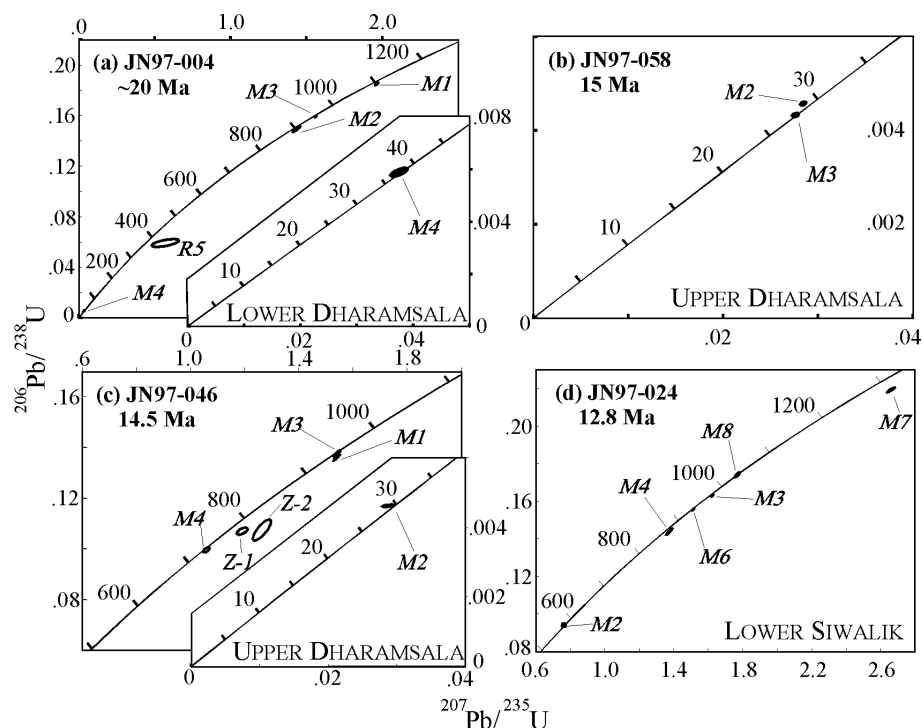
Fig. 4. U–Pb Concordia diagram of individual detrital monazite (m), zircon (z) and rutile (r) from Dharamsala Formation and Lower Siwalik sandstones, analysed by ID-TIMS. Sample numbers and depositional age refer to Figure 3. Insets show detail for young monazite ages. Ellipses represent 2σ error. Analysis numbers correspond to those in Table 1.

Table 2. *U-Th-Pb LA-PIMMS analytical data*

						Age (Ma)			
Analysis	^{232}Th (volts)	^{207}Pb*/^{206}Pb*	^{206}Pb†/^{238}U†	^{208}Pb†/^{232}Th†	^{232}Th‡/^{238}U‡	^{206}Pb/^{238}U	^{207}Pb/^{235}U	^{208}Pb/^{232}U	^{207}Pb/^{206}Pb
JN97-004 Sandstone from base of Lower Dharamsala formation (c. 20 Ma)									
g1	0.32 (4.0)	bd	0.1620 (2.8)	0.05477 (2.8)	65	968 ± 30	bd	1078 ± 37	bd
g2	0.946 (2.0)	bd	bd	0.001365 (1.3)	19	bd	bd	28 ± 1	bd
g3	0.706 (2.0)	bd	0.004853 (1.5)	0.001619 (1.7)	5	31 ± 1.0	bd	33 ± 1	bd
g4	1.11 (5.0)	bd	0.1613 (0.8)	0.04932 (2.2)	69	964 ± 16	bd	973 ± 29	bd
JN97-058A Sandstone from Upper Dharamsala formation (c. 15 Ma)									
g1	0.327 (18)	bd		0.002350 (11)	10	bd	bd	47 ± 5	bd
g2	3.85 (7.0)	0.06 (0.8)	0.08745 (5.2)	0.02527 (4.7)	21	540 ± 39	547 ± 40	504 ± 30	603
g3	1.77 (10)	bd	0.005615 (9.6)	0.001716 (11)	7	36 ± 4.0	bd	35 ± 4	bd
JN97-046 Sandstone from Upper Dharamsala formation (c. 14.5 Ma)									
g1	1.23 (18)	bd	0.1381 (16)	0.05166 (16)	51	834 ± 116	bd	1018 ± 167	bd
g2	1.15 (23)	bd	0.1272 (13)	0.03948 (13)	55	772 ± 159	bd	783 ± 113	bd
g3	0.661 (26)	0.0725 (1)	0.2256 (14)	0.06156 (14)	10	1311 ± 198	1186 ± 179	1207 ± 187	1000
JN97-024 Sandstone from the base of the Lower Siwalik formation (c. 12.8 Ma)									
g1	1.55 (15)	0.07575 (1)	0.2117 (15)	0.05889 (15)	20	1238 ± 198	1173 ± 188	1157 ± 190	1088
g2 (int)	1.68 (20)	0.08372 (10)	0.01193 (20)	0.007212 (20)	7	76 ± 16	130 ± 30	145 ± 31	1286
g2 scan 1	1.6 (2.0)	0.1003 (2)	0.02013 (2.0)	0.01275 (2.0)	7	128 ± 8	247 ± 16	256 ± 18	1629
g2 scan 2	1.92 (2.0)	0.0775 (2)	0.01183 (4.0)	0.007230 (4.0)	7	76 ± 5	120 ± 9	146 ± 11	1134
g2 scan 3	2.54 (2.0)	0.0744 (2)	0.006427 (4.0)	0.003303 (4.0)	7	41 ± 3	64 ± 5	67 ± 5	1052
g2 scan 4	0.92 (2.0)	0.0754 (2)	0.01674 (4.0)	0.01037 (4.0)	7	107 ± 7	161 ± 12	209 ± 16	1079
g2 scan 5	1.48 (2.0)	bd	0.004612 (4.0)	0.002410 (4.0)	7	30 ± 2	bd	49 ± 4	bd

bd indicates unreliable data due to low signal intensity when ^{206}Pb or ^{207}Pb<160 µV. Errors are 1 standard error of the mean in percent for ratios and ^{232}Th(V) and 2 standard errors of the mean when expressed in Ma.
*Corrected for instrumental mass bias using Tl with a natural Tl composition of 2.3871 for ^{205}Tl/^{203}Tl.
†Calculated using measured ratio correct for combined laser and instrumental Pb/U and Pb/Th elemental fractionation by normalizing to the ^{206}Pb/^{238}U (or ^{208}Pb/^{232}Th) ratio of monazite standard of known age and ratio, as determined by ID-TIMS analysis.
‡Includes a correction for Th/U elemental fractionation.

were 80–110 µm in size; rounded to well rounded and flattened elliptical (bladed) to oblate in shape. Monazite rarely preserved their original crystal shape, having been substantially abraded during transport, however occasional grains preserved evidence of crystal facets and were more sub-angular (Table 1). Many of the grains are clear, but those which had been most
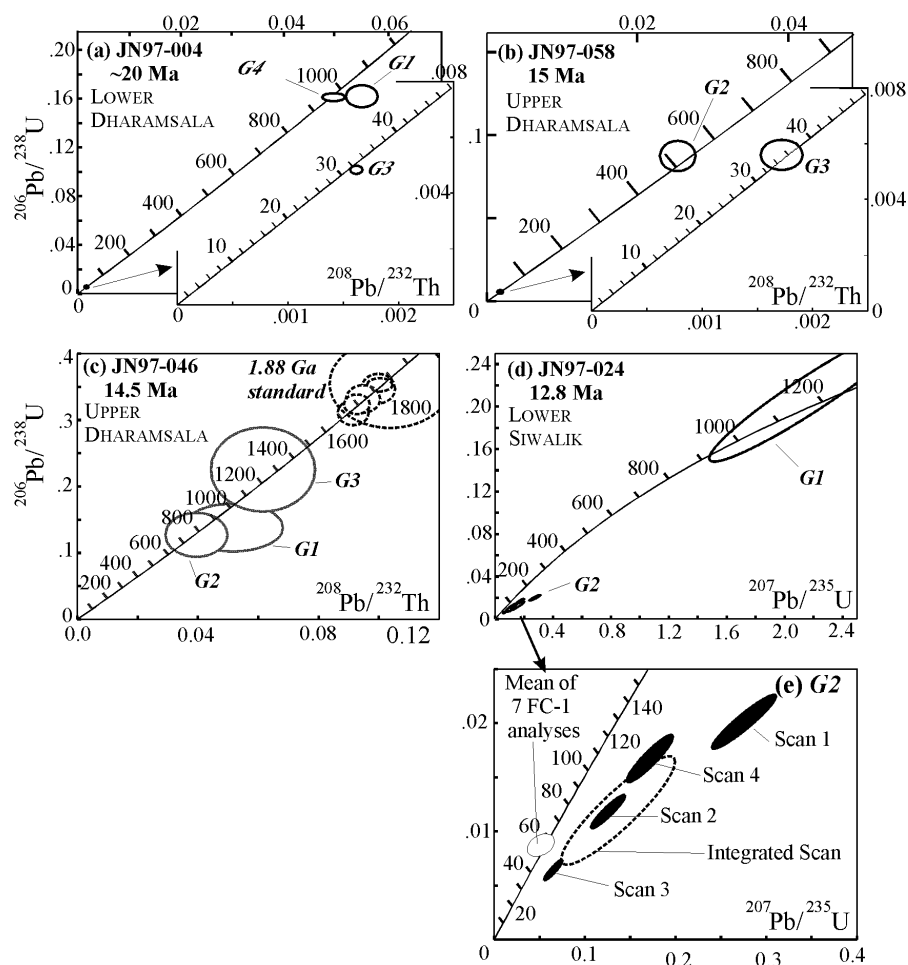
Fig. 5. U–Th–Pb Concordia diagrams of individual detrital monazite analysed by LA-PIMMS from Dharamsala Formation (**a–c**) and Lower Siwalik (**d–e**) sandstones. Analysis numbers correspond to those in Table 2. Note that (e) is a detail of grain 24G2 which shows the results of individual laser scans (solid fill) and the integrated scan values (dashed line), we interpret the variation between scans to represent a grain with a relict core (*c.* 500–1000 Ma) and young rim (*c.* 30 Ma). Analysis of standards run during data collection are shown (c) 1.88 Ga and (e) FC-1 (*c.* 54 Ma).

rounded by physical abrasion were dusty in appearance and a few grains have broken edges (a possible consequence of crushing). Of the zircon crystals chosen, one is euhedral and clear, the other smooth.

Most of the grains analysed show concordance to slight discordance; five grains out of 31 are discordant. Of the concordant results, the Lower Dharamsala, Upper Dharamsala and Lower Siwalik formations all contain 'Pre-Himalayan', >55 Ma ages (i.e. crystallized prior to collision and therefore related to the pre-collisional geological history) in the range *c.* 400–1300 Ma and (Figs 4 to 6). The Dharamsala Formation sandstones also contain Tertiary age grains of *c.* 28–37 Ma (ID-TIMS and LA-PIMMS analysis reveal a similar pattern of ages). The Lower Siwalik sample did not yield a concordant Himalayan grain but laser scans (Fig. 5e) on an individual grain suggest a young (*c.* 30–40 Ma) rim on an otherwise 'old' relict core (*c.* 500–1000 Ma) giving mixed ages as the grain was rastered during laser ablation. Furthermore, slight discordance in M4 from the Siwaliks (Fig. 4d) and grain morphology (equant, sub rounded, and faceted grain) may also be the result of younger rim on a predominantly old core.

Of the discordant results, grain M7 (Fig. 4d) is similar to zircons from the High Himalayan sequence analysed by Parrish & Hodges (1996) which were interpreted as having late Mesoproterozoic to Neoproterozoic overgrowths on Late Archaean to Palaeoproterozoic grains. Grain M5 (Fig. 4c) is interpreted as rutile owing to a U content of 9 ppm. Two of the

young grains exhibit reverse discordance (Scharer *et al.* 1984) attributed to excess ^{206}Pb (grain M2, Fig. 4b & M2, Fig. 4c).

The closure temperature of U–Th–Pb in monazite is thought to be in excess of *c.* 750°C (Spear & Parrish 1996). Monazite grows during prograde regional staurolite grade metamorphism ($525 \pm 50°$, Smith & Barreiro 1990; Foster *et al.* 2000) in pelitic schists resulting in its isotopic age recording the time of crystallization. The distinction between igneous and metamorphic monazite has been made on the basis of grain morphologies, but in this study, physical abrasion through erosion and reworking has generally destroyed original shapes. The U–Pb isotopic ages show that the rounded grains are all pre-Himalayan in age (Table 1). Those monazite grains with remnant crystal facets have Himalayan ages or Himalayan-age rims. We interpret these as metamorphic in origin because of the co-occurrence of detrital metamorphic minerals (e.g. garnet and rare staurolite) and medium grade metamorphic lithic fragments in the sediments, and the absence of sillimanite, which is found in the country rocks around the presently exposed Himalayan-age granites.

Discussion

Provenance

The pre-Himalayan history of the Himalayan tectonic units has been determined from whole rock Sm–Nd, Rb–Sr and U–Pb detrital zircon isotopic studies. These show that the
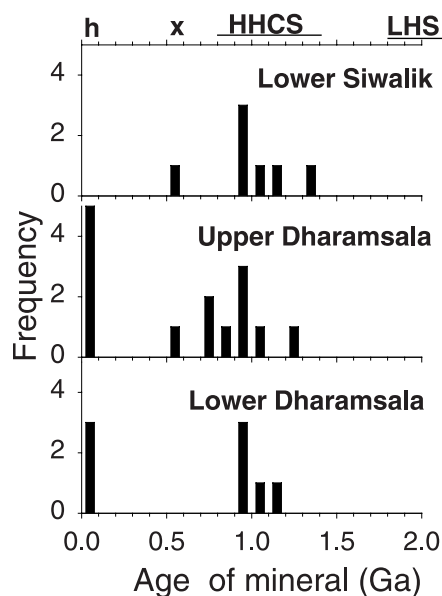
Fig. 6. Histograms showing distributions of concordant U–Pb, U–Th–Pb ages of detrital monazite and zircon from the Dharamsala and Lower Siwalik Formations. For comparison the range of ages of detrital zircons from metasediments of the High Himalayan Crystalline Series (HHCS) and Lesser Himalayan Series (LHS) are shown (Parrish & Hodges 1996; DeCelles *et al.* 2000), *h* is the time of Himalayan collision and *x* the time of intrusion of Cambro-Ordovician orthogneisses and granites.

Indus–Tsangpo suture zone, Tibetan Sedimentary Series, Lesser Himalayan Series and High Himalayan Crystalline Series were derived from crustal sources with distinctly different mantle-derivation ages, geochemistry and tectonic histories (France-Lanord *et al.* 1993; Parrish & Hodges 1996; Ahmad *et al.* 2000). The Sm–Nd and Rb–Sr isotopic compositions and detrital mineral populations of the Subathu Formation, Dagshai Formation, Kasauli Formation foreland basin sediments as well as mid-Miocene and younger sediments from the Bay of Bengal show that whereas the Indus–Tsangpo suture zone supplied sediment to the pre-mid-Eocene Subathu Formation, all the younger foreland basin sediments (late Oligocene and younger) were dominated by High Himalayan Crystalline Series sources (Najman *et al.* 2000).

Parrish & Hodges (1996) and DeCelles *et al.* (2000) showed that High Himalayan Crystalline Series rocks from Nepal, contain detrital zircon populations in metasediments of 0.8–1.0 Ga, up to 1.7 Ga and *c.* 500 Ma zircons from orthogneisses and granitic plutons, whereas Lesser Himalayan Series rocks from the same area were characterized by >1.6 to 2.6 Ga zircons. The majority of published U–Th–Pb monazite ages from the High Himalayan Crystalline Series metasediments and leucogranites give Tertiary ages (Simpson *et al.* 2000; Searle *et al.* 1999 and references therein). Only rarely are pre-Himalayan ages preserved. These are as relict cores (Harrison *et al.* 1995) giving discordant monazite ages with upper intercepts of *c.* 500 Ma interpreted as resulting from pre-Himalayan metamorphism and intrusion at 500 Ma (Walker *et al.* 1999).

The majority of the detrital monazites analysed in this study (Tables 1 & 2, Figs 4–6) have ages of between 0.8 and 1.3 Ga. Only one monazite grain (JN97-024) from the Lower Siwalik strata may incorporate an older component as inferred from its

discordance (Fig. 5d). These Meso-Neoproterozoic detrital monazites have not been particularly affected or 'reset' by Himalayan metamorphism, as is typical for monazite from High Himalayan Crystalline Series, yet share ages comparable to zircon in High Himalayan meta-sediments in the Langtang area, central Nepal (Parrish & Hodges 1996). We infer that they were derived from an unmetamorphosed (Tertiary) or lower grade equivalent of the present-day exposed High Himalayan Crystalline Series and are second-cycle detrital minerals. Such low-grade rocks with Nd–Sr isotope and trace element signatures characteristic of the High Himalayan Crystalline Series have been documented within the Lesser Himalayas of the Garhwal Himalayas (Ahmad *et al.* 2000). The two monazites and rutile grains with ages of *c.* 400–600 Ma (Fig. 6) may be derived from Cambro-Ordovician granitoids (Trevedi *et al.* 1984) or Precambrian meta-sediments affected by a Cambro-Ordovician metamorphism which provided the protolith and cover to the High Himalayan Crystalline Series (Pognante *et al.* 1990; Walker *et al.* 1999) and are presently exposed structurally above the High Himalayan Crystalline Series in Zanskar (Fig. 1).

There are no monazite ages (metamorphic or detrital) reported in the literature from rocks of the Lesser Himalayan Series. But, we assume that if they contain monazite, these monazites would preserve similar age population to Lesser Himalayan detrital zircons (i.e. *c.* 1.8–2.6 Ga, Fig. 6) (Parrish & Hodges 1996; DeCelles *et al.* 2000). There are no grains of this range in these samples (Fig. 6). At the present day, the Lesser Himalayan Series contributes (depending upon the catchment) between 20% and 50% of the solid load to rivers which drain the orogen (Galy 1999). The probability of missing grains from an older population, assuming an even density of the mineral and an erosional contribution of 20%, in a small sample size (e.g. out of 9 grains) is *c.* 13% (Dodson *et al.* 1988). These results, although speculative, when combined with bulk petrography and isotopic composition of the same sediments (White *et al.* 2000) suggest that the Lesser Himalayan Series is unlikely to form a significant part of the source in the early Miocene. Evidence for erosion of the Lesser Himalayas in NW India is, however, apparent from the Middle Siwalik Group at *c.* 9 Ma which contain conglomerates derived from the hangingwall of the Main Boundary Thrust (Meigs *et al.* 1995). The results from the Dharamsala Formation sandstones are in agreement with results from the Dumri sandstones of Nepal (DeCelles *et al.* 1998b) where the source is High Himalayan Crystalline Series and Tibetan Sedimentary Series. However for the Lower Siwalik sample our results contrasts with those of DeCelles *et al.* (1998a) who found a significant proportion of >*c.* 1.8 Ga zircons in Lower Siwalik rocks (<13 Ma) of Nepal and the proportion of these older zircons increased in the younger Siwalik units.

Tertiary ages

About one quarter of the monazites give Tertiary ages (Fig. 6) interpreted to indicate crystallization during the Himalayan metamorphism. Published Himalayan monazite ages lie in the range *c.* 44 to *c.* 12 Ma and 8–5 Ma (Hodges *et al.* 1996; Harrison *et al.* 1997; Searle *et al.* 1999; Foster *et al.* 2000; Simpson *et al.* 2000). Most of the published monazite ages are from leucogranites which form a small part of the outcrop
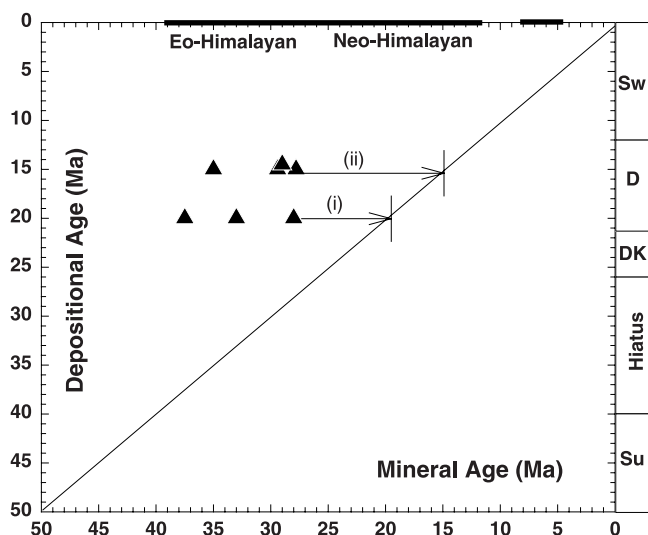
Fig. 7. Graph of mineral age versus depositional age for detrital monazite in Dharamsala Formation. A 1:1 line, where age of deposition equals mineral age is shown. Arrows between the time of crystallization of the youngest monazite to the arrival in the basin (i) deposition at 20 Ma and (ii) deposition at 15 Ma represents the delivery time and may be used to estimate the maximum cooling or exhumation rate. Solid lines at the top show the range of crystallization ages in metamorphic and igneous rocks of presently exposed High Himalayan Crystalline Series rocks. Boxes on the right show the division of sedimentary sequences in the North Indian Himalayan foreland, (Su) marine Subathu formation, one sample from this formation conceded no monazite grains, (DK) Dagshai–Kasauli formations, one sample from the Lower Dagshai conceded no monazite grains, (D) Dharamsala formation, this study, note that the deposition of exhumed Eo-Himalayan metamorphic rock in these sediments was co-eval with Neo-Himalayan metamorphism, (Sw) Siwalik group, no data are yet available.

area. Monazites from metamorphic rocks (including deformed orthogneisses and migmatitic leucosomes) are likely to be volumetrically dominant and have inferred crystallization ages of *c.* 44–36 Ma and 34–24 Ma (Foster *et al.* 2000), 36 Ma, *c.* 30 Ma, and 22.5 Ma (Hodges *et al.* 1996), *c.* 32 Ma and *c.* 23 Ma (Simpson *et al.* 2000), and 18 and 20 Ma (Parrish & Hodges 1996).

The detrital monazites, which have ages between 37 Ma (and possibly older) and 28 Ma, are derived from the Eo-Himalayan (latest Eocene–Oligocene) part of the metamorphic cycle (Fig. 7). With a high closure temperature, monazite may record different points in a metamorphic cycle. Initial monazite growth at staurolite facies conditions (*c.* 525°C, Smith & Barreiro 1990) takes place during prograde conditions. The 37 Ma and 28 Ma ages of the detrital grains is consistent with their crystallizing during the same prograde cycle as dated by Sm–Nd isotopic analyses of garnet cores and rims from High Himalayan Crystalline Series rocks of Zanskar and Garhwal with ages between *c.* 40 Ma and 25 Ma (Prince *et al.* 1999; Vance & Harris 1999) and also with U–Th–Pb ages of *in situ* monazite inclusions within garnet (44–36 Ma) and monazite in the matrix (34–25 Ma) from metamorphic rocks of Garhwal (Foster *et al.* 2000). The extent to which monazite may continue to crystallize during the subsequent metamorphic evolution is uncertain and possibly related to availability of apatite, bulk composition and/or changes in the fluid regime (Simpson *et al.* 2000). However melting and crystallization of the melts as leucosomes, or their segregation into leucogranites, forms new monazite late in the metamorphic cycle such as that dated in the Himalayan leucogranites or sillimanite facies migmatites (e.g. the 22.5 Ma age reported by Hodges *et al.* 1996 and 18 and 20 Ma ages reported by Parrish & Hodges 1996).

The detrital monazites with ages of *c.* 37 Ma and *c.* 28 Ma deposited at 20 Ma and 15 Ma and rim age of *c.* 30(?) Ma deposited at 12.8 Ma imply that some of the rocks that underwent Eo-Himalayan metamorphism between 44 and 25 Ma reached the surface by *c.* 20 Ma (Fig. 7). The lack of younger *c.* 20 Ma monazites in the lower Siwaliks is unsurprising given that the migmatitic rocks and leucogranites are mainly confined to sillimanite facies High Himalayan Crystalline Series rocks and detrital sillimanite does not appear until the Upper Siwaliks in India *c.* 5–7 Ma (Chaudhri 1975; Sorkhabi & Arita 1997 and references therein). In Nepal sillimanite appears towards the top of the Lower Siwalik sub-group dated at *c.* 11 Ma (DeCelles *et al.* 1998*a*) (Fig. 2).

The evolution of detrital metamorphic minerals and monazite ages is consistent with the predictions of one-dimensional models of over-thickened crust in which less deeply buried rocks are heated less and exposed earlier (cf. England & Richardson 1977). Collision and initial burial took
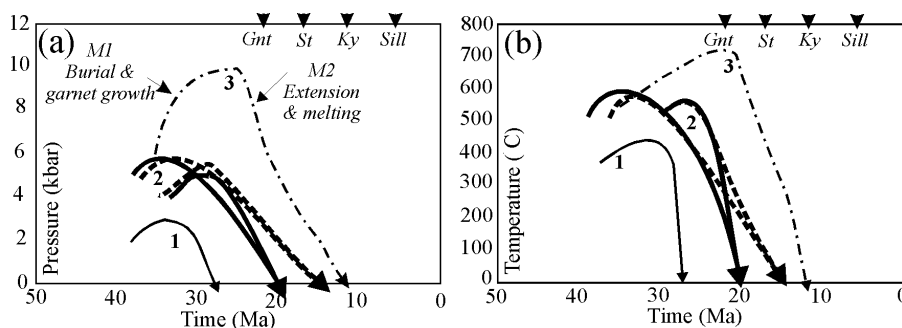

Fig. 8. Pressure–time (**a**) and temperature–time (**b**) paths. 1, Trajectory (thin line) for rocks sub-garnet grade, which were eroded by Dagshai times (based upon mica ages, Najman *et al.* 1997). 2, Trajectories (thick solid line, Upper Dharamsala; thick dash line, Lower Dharamsala) from garnet–staurolite-grade metamorphism (crystallization of monazite) to deposition in Dharamsala formation. 3, Trajectory (dash dot line) for presently exposed High Himalayan kyanite-grade pelites from Zanskar (Searle *et al.* 1999; Vance & Harris 1999). The time of first appearance in the detrital record of metamorphic index minerals is shown.

place at 50–45 Ma (Rowley 1996). Sub-garnet grade rocks were exhumed and eroded by Dagshai times (Najman & Garzanti 2000) (trajectory 1, Fig. 8). The oldest garnet grade rocks crystallized at *c.* 550°C and at *c.* 0.6 GPa *c.* 10–20 Ma after burial (Vance & Mahar 1998; Vance & Harris 1999) were exposed 30 Ma after initial burial (trajectory 2, Fig. 8). Kyanite facies rocks reached 650°C at 1 GPa *c.* 25 Ma after burial before decompressing into the sillimanite field (20 Ma) and being exposed *c.* 40 Ma after burial (Sorkhabi & Arita 1997; Vance & Harris 1999; Foster *et al.* 2000) (trajectory 3, Fig. 8). The highest-grade rocks exposed today were heated to *c.* 800°C at *c.* 1.2 GPa, 30 Ma after burial before decompressing into the sillimanite field before and being exposed *c.* 40–45 Ma after burial today (trajectory not shown) (Dezes *et al.* 1999). However such a one dimensional evolution is certain to be an oversimplification as spatially and temporally variable exhumation rates are implied by both cooling rates (Searle *et al.* 1999) and by the duration of the deposition of key index assembly minerals (e.g. staurolite from 18 Ma to present day). At present there are insufficient monazite ages to constrain the undoubtedly more complex two- or three-dimensional evolution of the over-thrust crust where exhumation was controlled by a combination of thrusting and migration of thrusts, normal faulting and erosion.

Conclusions

Detrital monazite ages provide information on both source and metamorphic evolution of the Himalayan tectonic units. The detrital monazites from a section of the Dharamsala and Lower Siwaliks in NW India dated by magneto-stratigraphy to between *c.* 20 and 12.8 Ma preserve *c.* 0.7–1.3 Ga ages characteristic of High Himalayan Crystalline Series precursors, rare 600–400 Ma ages from Cambro-Ordovician plutons, and Tertiary Himalayan metamorphic ages. The Himalayan metamorphic monazite ages apparently date the pro-grade part of the Eo-Himalayan metamorphic phase (40–25 Ma) when monazite ages, garnet core and rim Sm–Nd ages and chemical zoning indicate that the thrust pile was being buried and heated (Vance & Mahar 1998; Vance & Harris 1999; Walker *et al.* 1999; Foster *et al.* 2000). Some of the metamorphic rocks were eroded as early as 20 Ma whereas others are exposed at the surface today. The lack of 20 Ma monazites from the Neo-Himalayan phase of decompression and melting as detritus in the Dharamsala and Lower Siwalik sequence is consistent with the absence of detrital sillimanite prior to *c.* 11 Ma.

References

AHMAD, T., HARRIS, N., BICKLE, M., CHAPMAN, H., BUNBURY, J. & PRINCE, C. 2000. Isotopic constraints on the structural relationships between the Lesser Himalayan Series and the High Himalayan Crystalline Series, Garhwal Himalaya. *Geological Society of America Bulletin*, **112**, 324–350.

AVOUAC, J.P. & TAPPONNIER, P. 1993. Kinematic model of active deformation in Central Asia. *Geophysical Research Letters*, **20**, 895–898.

BURBANK, D.W., BECK, R. A. & MULDER, T. 1996. The Himalayan Foreland Basin. *In:* YIN, A. & HARRISON, T.M. (eds) *The Tectonic Evolution of Asia.* Cambridge University Press, 149–188.

CANDE, S.C. & KENT, D.V. 1995. Revised calibration of the geomagnetic polarity timescale for the late Cretaceous and Cenozoic. *Journal of Geophysical Research*, **100**, 6093–6095.

CHAUDHIRI, R.S. 1975. Sedimentology and Genesis of the Cenozoic Sediments of Northwestern Himalayas (India). *Geologische Rundschau*, **64**, 958–977.

COPELAND, P., HARRISON, T.M., HODGES, K.V., MARUEJOL, P., LE FORT, P. & PECHER, A. 1991. An early Pliocene thermal disturbance of the Main Central Thrust, central Nepal; implications for Himalayan tectonics. *Journal of Geophysical Research*, **B96**, 8475–8500.

DECELLES, P.G., GEHRELS, G.E., QUADE, J., OJHA, T.P., KAPP, P.A. & UPRETI, B.N. 1998*a*. Neogene foreland basin deposits, erosional unroofing, and the kinematic history of the Himalayan fold-thrust belt, western Nepal. *Geological Society of America Bulletin*, **110**, 2–21.

DECELLES, P.G., GEHRELS, G.E., QUADE, J. & OJHA, T.P. 1998*b*. Eocene-Early Miocene foreland basin development and the history of Himalayan thrusting, western and central Nepal. *Tectonics*, **17**, 741–765.

DECELLES, P.G., GEHRELS, G.E., QUADE, J., LAREAU, B. & SPURLIN, M. 2000. Tectonic Implications of U–Pb Zircon Ages of the Himalayan Orogenic Belt in Nepal. *Science*, **288**, 497–499.

DEZES, P.J., VANNEY, J-C., STECK, A., BUSSY, F. & COSCA, M. 1999. Synorogenic extension: Quantitative constraints on the age and displacement of the Zanskar shear zone (northwest Himalaya). *Geological Society of America Bulletin*, **111**, 364–374.

DODSON, M.H., COMPSTON, W., WILLIAMS, I.S. & WILSON, J.F. 1988. A search for ancient detrital zircons in Zimbabwean sediments. *Journal of the Geological Society, London*, **145**, 977–983.

ENGLAND, P.C. & RICHARDSON, S.W. 1977. The influence of erosion upon the mineral facies of rocks from different metamorphic environments. *Journal of the Geological Society, London*, **134**, 201–213.

FOSTER, G., KINNY, P., VANCE, D., PRINCE, C. & HARRIS, N. 2000. The significance of monazite U–Th–Pb age data in metamorphic assemblages; a combined study of monazite and garnet chronometry. *Earth and Planetary Science Letters*, **181**, 327–340.

FRANCE-LANORD, C., DERRY, L. & MICHARD, A. 1993. Evolution of the Himalaya since Miocene time: isotopic and sedimentological evidence from the Bengal Fan. *In:* TRELOAR, P.J. & SEARLE, M.P. (eds) *Himalayan Tectonics.* Geological Society, London. Special Publications, **74**, 603–621.

FUCHS, G. 1982. The geology of the Pin valley in Spiti, H.P., India. *Jahrbuch der Geologischen Bundesanstalt*, **124**, 325–359.

GAETANI, M. & GARZANTI, E. 1991. Multicyclic history of the Northern India Continental margin (northwestern Himalaya). *The American Association of Petroleum Geologists Bulletin*, **75**, 1427–1446.

GALY, A. 1999. *Etude géochimique de l'érosion actuelle de la chaine himalayenne.* PhD thesis. Institut National Polytechnique de Lorraine, Nancy.

GANSSER, A. 1964. *Geology of the Himalayas.* Interscience Publishers, London.

GARZANTI, E. & VAN HAVER, T. 1988. The Indus clastics: forearc basin sedimentation in the Ladakh Himalaya (India). *Sedimentary Geology*, **59**, 237–249.

GODIN, L., BROWN, R.L., HANMER, S. & PARRISH, R.R. 1999. Back folds in the core of the Himalayan Orogen: An alternative interpretation. *Geology*, **27**, 151–154.

GUILLOT, S., COSCA, M., ALLEMAND, P. & LE FORT, P. 1999. Contrasting metamorphic and geochronologic evolution along the Himalayan belt. *In:* MACFARLANE, A., SORKHABI, R.B. & QUADE, J. (eds) *Himalaya and Tibet: mountain roots to mountain tops.* Geological Society of America Special Papers, **328**, 117–128.

HARRIS, N. & AYERS, M. 1998. The implications of Sr-isotope disequilibrium for rates of prograde metamorphism and melt extraction in anatectic terrains. *In:* TRELOAR, P.J. & O'BRIAN, P. (eds) *What Drives Metamorphism and Metamorphic Reactions?* Geological Society, London. Special Publications, **138**, 171–182.

HARRISON, T.M., MCKEEGAN, K.D. & LEFORT, P. 1995. Detection of inherited monazite in the Manaslu leucogranite by [208]Pb/[232]Th ion microprobe dating: Crystallisation age and tectonic implications. *Earth and Planetary Science Letters*, **133**, 271–282.

HARRISON, T.M., RYERSON, F.J., LE FORT, P., YIN, A., LOVERA, O.M. & CATLOS, E.J. 1997. A Late Miocene-Pliocene origin for the Central Himalayan inverted metamorphism. *Earth and Planetary Science Letters*, **146**, 1–7.

HODGES, K.V. 2000. Tectonics of the Himalaya and southern Tibet from two perspectives. *Geological Society of America Bulletin*, **112**, 324–350.

HODGES, K.V., PARRISH, R.R. & SEARLE, M.P. 1996. Tectonic evolution of the central Annapurna Range, Nepalese Himalaya. *Tectonics*, **15**, 1264–1291.

HUBBARD, M.S. & HARRISON, T.M. 1989. ^{40}Ar/^{39}Ar Age constraints on deformation and metamorphism in the Main Central Thrust zone and the Tibetan Slab, Eastern Nepal Himalaya. *Tectonics*, **8**, 865–880.

KARUNAKARAN, C. & RANGA RAO, A. 1979. Status of exploration for hydrocarbons in the Himalayan region-contributions to stratigraphy and structure. *Himalayan Geology Seminar-1976*. Geological Survey of India, Miscellaneous Publications, **41**, 1–66.

LE FORT, P., CUNEY, M., DENIEL, C., FRANCE-LANORD, C., SHEPPARD, S.M.F., UPRETI, B.N. & VIDAL, P. 1987. Crustal generation of the Himalayan leucogranites. *Tectonophysics*, **134**, 39–57.

MATHUR, N.S. 1978. Biostratigraphical aspects of the Subathu Formation, Kumaun Himalaya. *Recent Researches in Geology*, **12**, 81–90.

MEIGS, A.J., BURBANK, D.W. & BECK, R.A. 1995. Middle-late Miocene (>10 Ma) formation of the Main Boundary thrust in the western Himalaya. *Geology*, **23**, 423–426.

METCALFE, R.P. 1993. Pressure, temperature, and time constraints on metamorphism across the Main Central Thrust zone and the High Himalayan Slab in the Garhwal Himalaya. *In:* TRELOAR, P.J. & SEARLE, M.P. (eds) *Himalayan Tectonics*. Geological Society, London. Special Publications, **74**, 525–540.

NAJMAN, Y. & GARZANTI, E. 2000. Reconstructing early Himalayan tectonic evolution and paleogeography from Tertiary foreland basin sediments, Northern India. *Geological Society of America Bulletin*, **112**, 435–449.

NAJMAN, Y., CLIFT, P., JOHNSON, M.R.W. & ROBERTSON, A.H.F. 1993. Early stages of foreland basin evolution in the Lesser Himalaya, N. India. *In:* TRELOAR, P.J. & SEARLE, M.P. (eds) *Himalayan Tectonics*. Geological Society, London. Special Publications, **74**, 541–558.

NAJMAN, Y., PRINGLE, M.S., JOHNSON, M.R.W., ROBERTSON, A.H.F. & WIJBRANS, J.R. 1997. Laser ^{40}Ar/^{39}Ar dating of single detrital muscovite grains from early foreland-basin sedimentary deposits in India: Implications for early Himalayan evolution. *Geology*, **25**, 535–538.

NAJMAN, Y., BICKLE, M.J. & CHAPMAN, H.J. 2000. Early Himalayan exhumation: Isotopic constraints from the Indian foreland basin. *Terra Nova*, **12**, 28–34.

NOBLE, S.R., TUCKER, R.D. & PHARAOH, T.C. 1993. Lower Paleozoic and Precambrian igneous rocks from Eastern England, and their bearing on late Ordovician closure of the Tornquist Sea: Constraints from U–Pb and Nd isotopes. *Geological Magazine*, **130**, 835–846.

PARRISH, R.R. & HODGES, K.V. 1996. Isotopic constraints on the age and provenance of the Lesser and Greater Himalayan sequences, Nepalese Himalaya. *Geological Society of America Bulletin*, **108**, 904–911.

PARRISH, R.R., RODDICK, J.C., LOVERIDGE, W.D. & SULLIVAN, R.S. 1987. Uranium-lead analytical techniques at the Geochronological Labratory. *Radiogenic age and isotopic studies report 1*. Geological Survey of Canada Papers, **87-2**, 3–7.

PARRISH, R.R., NOWELL, G., NOBLE, S.R., HORSTWOOD, M., TIMMERMANN, H., SHAW, P. & BOWEN, I. 1999. LA-PIMMS: A new method of U-Th-Pb geochronology using micro-sampling techniques. *Terra Abstracts*, **11**, 799.

POGNANTE, U., CASTELLI, D., BENNA, P., GENOVESE, G., OBERLI, F., MEIER, M. & TONARINI, S. 1990. The crystalline units of the High Himalayas in the Lahul-Zanskar region (northwest India): metamorphic-tectonic history and geochronology of the collided and imbricated Indian plate. *Geological Magazine*, **127**, 101–116.

POWERS, P.M., LILLIE, R.J. & YEATS, R.S. 1998. Structure and shortening of the Kangra and Dehra Dun re-entrants, Sub-Himalaya, India. *Geological Society of America Bulletin*, **110**, 1010–1027.

PRINCE, C.I., FOSTER, G., VANCE, D., HARRIS, N. & BAKER, J. 1999. The Thermochronology of the High Himalayan Crystallines in the Garhwal Himalaya; Prograde history of a poly metamorphic slab. *Terra Nostra*, **99/2**, 119–120.

RAIVERMAN, V. & SESHAVATARAM, B.T.V. 1965. On mode of deposition of Subathu and Dharamsala sediments in the Himalayan foothills in Punjab and Himachal Pradesh. *Wadia Commemorative Volume*, 556–571.

RAIVERMAN, V., KUNTE, S.V. & MUKHERJEA, A. 1983. Basin Geometry, Cenozoic Sedimentation and Hydrocarbon Prospects in North Western Himalaya and Indo-Gangetic Plains. *Petroleum Asia Journal*, **6**, 76–86.

ROWLEY, D.B. 1996. Age of initiation of collision between India and Asia: A review of stratigraphic data. *Earth and Planetary Science Letters*, **145**, 1–13.

SANGODE, S.J., KUMAR, R. & GHOSH, S.K. 1996. Magnetic polarity stratigraphy of the Siwalik sequence of Haripur area (H.P.) NW Himalaya. *Journal of the Geological Society of India*, **47**, 683–704.

SCHARER, U., RONG-HUA, X. & ALLEGRE, C.J. 1984. U–Pb geochronology of Gangdese (Transhimalaya) plutonism in the Lhasa-Xigaze region, Tibet. *Earth and Planetry Science Letters*, **69**, 311–320.

SEARLE, M.P. 1983. Stratigraphy, structure and evolution of the Tibetan-Tethys zone in Zanskar and the Indus suture zone in the Ladakh Himalaya. *Transactions of the Royal Society of Edinburgh: Earth Sciences*, **73**, 205–219.

SEARLE, M.P., PARRISH, R.R., HODGES, K.V., HURFIELD, A., AYRES, M.W. & WHITEHOUSE, M.J. 1997. Shisha Pangma Leucogranite, South Tibetan Himalaya: Field Relations, Geochemistry, Age, Origin and Emplacement. *Journal of Geology*, **105**, 295–317.

SEARLE, M.P., WATERS, D.J., DRANSFIELD, M.W., STEPHENSON, B.J., WALKER, C.B., WALKER, J.D. & REX, D.C. 1999. Thermal and mechanical models for the structural and metamorphic evolution of the Zanskar High Himalaya. *In:* MAC NIOCAILL, C. & RYAN, P.D. (eds) *Continental Tectonics*. Geological Society, London. Special Publications, **164**, 139–156.

SIMPSON, R.L., PARRISH, R.R., SEARLE, M.P. & WATERS, D.J. 2000. Two episodes of monazite crystallisation during metamorphism and crustal melting in the Everest region of the Nepalese Himalaya. *Geology*, **28**, 403–406.

SMITH, H.A. & BARREIRO, B. 1990. Monazite U-Pb dating of staurolite grade metamorphism in pelitic schists. *Contributions to Mineralogy and Petrology*, **105**, 602–615.

SORKHABI, R.B. & ARITA, K. 1997. A new method of estimating denudation rates of the High Himalaya based on metamorphic index minerals in the Siwalik molasse. *Journal of the Geological Society of India*, **50**, 691–696.

SPEAR, F.S. & PARRISH, R.R. 1996. Petrology and cooling rates of the Valhella Complex, British Columbia, Canada. *Journal of Petrology*, **37**, 733–765.

STEPHENSON, B.J., WATERS, D.J. & SEARLE, M.P. 2000. Inverted metamorphism and the Main Central Thrust: field relations and thermobarometric constraints from the Kishtwar Window, NW Indian Himalaya. *Journal of Metamorphic Geology*, **18**, 571–590.

THAKUR, V.C. 1998. Structure of the Chamba nappe and position of the Main Central Thrust in Kashmir Himalaya. *Journal of Asian Earth Sciences*, **16**, 269–282.

TREVEDI, J.R., GOPALAN, K. & VALDIYA, K.S. 1984. Rb–Sr ages of granitic rocks within the Lesser Himalayan nappes, Kumaun, India. *Journal of the Geological Society of India*, **25**, 641–654.

VALDIYA, K.S. 1980. *Geology of Kumaun Lesser Himalaya*. Dehra Dun, India.

VALDIYA, K.S. & BHATIA, S.B. (EDS) 1980. *Stratigraphy and Correlations of Lesser Himalayan Formations*. Hindustan Publishing Corporation, India.

VANCE, D. & HARRIS, N. 1999. Timing of prograde metamorphism in the Zanskar Himalaya. *Geology*, **27**, 395–398.

VANCE, D. & MAHAR, E. 1998. Pressure-temperature paths from P-T psuedo-sections and zoned garnets: Potential, pitfalls and examples from the Zanskar Himalaya, NW India. *Contributions to Mineralogy and Petrology*, **132**, 225–245.

WALKER, J.D., MARTIN, M.W., BOWRING, S.A., SEARLE, M.P., WATERS, D.J. & HODGES, K.V. 1999. Metamorphism, melting and extension: Age constraints from the High Himalayan Slab of Southeast Zanskar and Northwest Lahaul. *The Journal of Geology*, **107**, 473–495.

WHITE, N., GARZANTI, E. & PRINGLE, M. *et al.* 2000. The provenance of the Dharamsala Formation. *In:* HONGZHEN, W. (ed.) *Earth Science Frontiers*. 15th Himalaya–Karakorum–Tibet Workshop, Chengdu, China, 62–63.